Journal of Porous Materials 9: 211–219, 2002

Pore Structure and Permeability of an Alumina Fiber Filter Membrane for Hot Gas Filtration

J.A. FERNANDO AND D.D.L. CHUNG
Composite Materials Research Laboratory, University at Buffalo, The State University of New York, Buffalo, NY 14260-4400, USA

Revised May 21, 2002

Abstract. The pore structure and permeability of an alumina-fiber-based hot gas filter membrane containing an acid phosphate binder were characterized using capillary flow porometry. The smallest pore diameter was 1.24 ± 0.06 μm; the largest pore diameter (bubble point pore diameter) was 23 ± 1 μm. The pore size distribution was narrow, with almost all pores ranging from 2 to 4 μm, and the mean flow pore size 2.6 ± 0.1 μm. The Darcy permeability constant for air through the membrane was (114 ± 6) × 10^{-9} cm^2.

Keywords: membrane, alumina fiber, filter, pore size, porosity

1. Introduction

The use of highly porous and strong ceramic materials is increasing in applications such as hot gas filtration [1–3]. Lightweight, rigid, fibrous ceramic materials, in particular, have considerable potential for specialty filtration applications because of their thermal, electrical and acoustic properties [3]. Types of hot gas filtration applications include processes such as coal combustion, coal gasification, incineration, catalytic recovery and processing, and chemical and petrochemical processing.

Studies have shown that aluminosilicates such as mullite and cordierite, alumina, titania and silicon carbide would be good candidate materials for the manufacture of ceramic membrane filters [2]. In our earlier work [1], we demonstrated that even though the binder system constitutes only a small percentage of the fibrous filtration medium, it is critical to the mechanical properties and filtrate flow characteristics. In that study, the mechanical properties and pressure drop characteristics of alumina fiber based filter membranes made using colloidal silica, colloidal alumina and a non-commercial acid phosphate binder were evaluated and compared. It was demonstrated that filter membranes containing 9 to 10 wt% of the acid phosphate binder exhibited the lowest pressure drop in comparison to membranes with other binders while having the highest flexural and compressive strengths. Microscopy also showed an important characteristic of the binding mechanism of the acid phosphate binder when used at the optimum levels, that is that the acid phosphate caused the fibers to bond at their junctions only, whereas colloidal alumina and colloidal silica binders caused free binder particles within the fiber network. This fact is important because the way a binder acts to hold the fiber structure together also impacts the pore structure, pore size and pore size distribution [4]. These parameters, in turn, impact the filtration characteristics.

The primary function of hot gas filters in many of the applications mentioned above is to remove fine particulate materials from exhaust gases that are at elevated temperatures. The effectiveness of fibrous filter membranes for removing fine particulate materials depend on a number of factors, including fiber diameter, packing density, fiber orientation and velocity and particulate loading in the fluid stream [5]. Therefore, understanding the nature of the porosity and thereafter being able to tailor the filter membranes with better filtration characteristics for specific industrial applications

is important for the continued development of this technology.

A key need in such research is improving methods to characterize fundamental properties such as pore size, pore structure, pore size distribution, surface area and tortuosity. Although methods for the characterization of porous media, such as nitrogen adsorption-desorption and mercury intrusion are well known and widely accepted, such methods are limited in their ability to accurately characterize fibrous ceramic membrane materials [6–8].

Mercury porosimetry, in particular, is frequently used to characterize the pore structure of ceramic materials. This method is based on the measurement of the mercury uptake into the previously evacuated porous materials under increasing pressure of mercury. An obvious disadvantage to the mercury porosimetry method is that it uses highly toxic liquid mercury at very high pressures. The pressure required to completely infiltrate a porous body can be significant and will sometimes approach the crushing strength of the porous body (400 MPa to fill pores with radii of 1.5 nm [9]). Another drawback of the mercury porosimetry method is that it cannot measure the constricted size of a pore available for permeation and furthermore, cannot distinguish between dead-end pores and pores available for permeation [10, 11].

In the present study we used a characterization technique called capillary flow porometry to characterize the porosity of an alumina-fiber-based filter membrane material made using an acid phosphate binder. Using this technique we were able to determine some key parameters that are important for the filtration application such as the largest and smallest pore size, pore size distribution, and permeability.

2. Background on Characterization Technique

Although not commonly used to characterize porous ceramic materials, methods similar to the capillary flow porometry technique have been used for many years to characterize pore size distributions in various porous materials and membranes [12–17]. No uniform nomenclature exists, and various names are used for related tests, such as Coulter porosimetry, bubble point test, permporometry, biliquid permporometry and thermoporometry, just to name a few. In fact, the abovementioned methods are rather similar and rely on the same basic physical principle, i.e., the displacement of a wetting liquid.

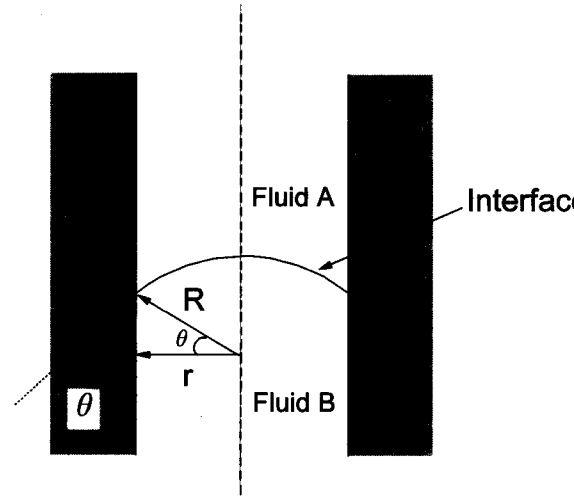

Figure 1. Schematic representation of the interfacial meniscus in a cylindrical pore in a membrane.

Figure 1 shows schematically a cylindrical pore in the cross-sectional view of a membrane. The membrane is wetted with a liquid which is held in the pores by capillary forces (fluid A). Another less wetting fluid (fluid B), liquid or gas, acts at increased pressure on one side of the membrane (bottom side of Fig. 1) and eventually displaces the former. The pressure difference Δp needed to expel the former liquid from a pore with radius r is given by Laplaces' equation [7]:

$$\Delta p = 2\gamma H, \tag{1}$$

where γ is the interfacial tension of the fluid-fluid system, and H is the mean curvature of the meniscus. The radius of the meniscus, R, relates to the pore radius, r, via the contact angle, θ, of the fluid-fluid membrane system, as illustrated in Fig. 1. In case of a spherical meniscus in a cylindrical pore, the principal curvature $c_1 = c_2 = 1/R$, and the mean curvature can be expressed as, $H = (c_1 + c_2)/2 = 1/R = \cos\theta/r$.

The solid-liquid interface free energy of a wetting liquid is lower than the solid-gas interface free energy. Therefore, filling of pores occurs spontaneously, but a non-reactive gas under pressure is required to force the liquid out of the pores. The pressure difference, Δp, required to displace the liquid at any location in the pore can be obtained by equating the work done by the gas to the increase in interface free energy [8].

$$\Delta p = (\gamma \cos\theta)\left(\frac{dS}{dV}\right), \tag{2}$$

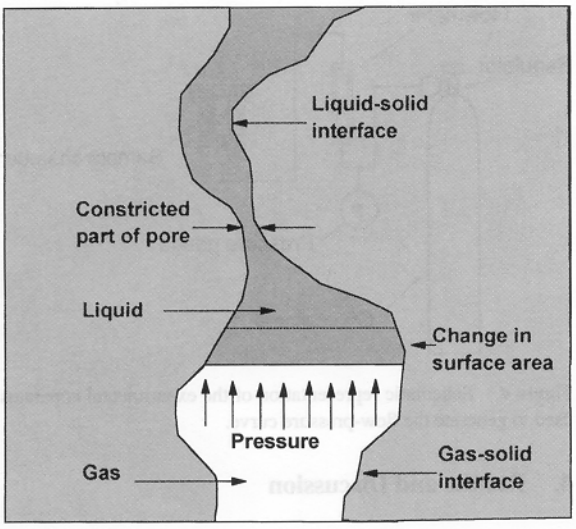

Figure 2. Schematic representation of a pore showing the variation in pore size along its length and the constricted pore size.

where dV is the incremental volume of gas in the pore and dS is the incremental solid-gas interface area due to dV (Fig. 2).

The quantity dS/dV is inversely related to the pore size [11]. The diameter D at a given location in the pore is defined as the diameter of a cylinder such that,

$$\left(\frac{dS}{dV}\right)_{\text{pore}} = \left(\frac{dS}{dV}\right)_{\text{cylinder}} \tag{3}$$

The (dS/dV) of a cylindrical pore of diameter D is $(4/D)$. Therefore, rearranging Eq. (2) and substituting the term for diameter of the cylindrical pore, D, one gets

$$D = (4\gamma \cos\theta)/\Delta p \tag{4}$$

It has been shown that $\cos\theta$ is close to one for wetting liquids with low surface tension. Therefore, for low surface tension liquids [8, 11],

$$D = \frac{4\gamma}{\Delta p} \tag{5}$$

Until the pressure difference across the membrane reaches the capillary pressure of the largest pores, fluid A (Fig. 1) acts like a barrier and no flow can occur. After increasing the pressure over this limit, fluid A is expelled from the largest pores, allowing the other fluid, B, to permeate. By successively increasing the pressure, smaller and smaller pores are opened for permeation of fluid B [15].

3. Experimental Methods

3.1. *Filter Membrane Fabrication*

Alumina fiber filter membranes containing 9.0 to 9.5 wt% of a non-commercial acid phosphate binder were fabricated using a wet forming method. The binder solution used for fabricating the filter membrane was prepared by mixing one part aluminum hydroxide ($Al(OH)_3$, obtained from Aldrich Chemical Co., Milwaukee, Wisconsin) with phosphoric acid (H_3PO_4, 85% Technical Grade, also obtained from Aldrich Chemical Co.), such that the solution had a P/Al atom ratio of 23 [1]. The phosphoric acid was stirred and heated to approximately 150°C. Then aluminum hydroxide was slowly mixed in and allowed to dissolve completely.

Information about the alumina fiber (Saffil, ICI Performance Chemicals, Cheshire, U.K.) used in this study is summarized in Table 1. The dimensions and density of the specimens are shown in Table 2.

3.2. *Porosity Characterization*

A Capillary Flow Porometer (Model 1200 AEX, made by Porous Materials, Inc., Ithaca, New York) was used in this study. A block diagram shown in Fig. 3 describes the apparatus. The pore characteristics of the filter membrane material were determined by first soaking the membrane in the wetting liquid to fill all the pores. The sample was then held between two orings such that the gas flows through pores in the thickness direction of the sample (Fig. 4). The applied gas

Table 1. Properties of the Al_2O_3 fiber filter media.

Trade name	Saffil
Grade	RF milled
Mean diameter (μm)	3[a]
Mean length (μm)	115
Density (kg/m^3)	3300[a]
Tensile strength (MPa)	1000 to 2000[a]
Crystal phase	δ alumina[a]
Melting point (°C)	>2000[a]

[a]From Ref. [18].

Table 2. Physical characteristics of the Al_2O_3 fiber filter membrane.

Specimen thickness (mm)	18.5 ± 0.5
Specimen diameter (mm)	40.0 ± 0.5
Density (kg/m^3)	255.1 ± 5.2

pressure on one side of the sample forces out the wetting liquid from the pores. A wetting liquid called Galden HT 230 (made from fluorocarbons and perfluorinated polyethers by Brenntag N.V., Deerlijk, Belgium) having a surface tension of 15.9×10^{-8} mN/m was used in this study. Air was used as the gas phase to displace the wetting liquid from the pores of the filter membrane.

The Capillary Flow Porometer monitors both pressure and flow and records these in a pressure versus flow graph for wet and dry starting samples. At low gas pressures the flow rate is zero. Flow starts at the pressure that is sufficient to clear some of the pores. This pressure is called the bubble point pressure [6]. As the pressure increases, more pores get emptied and the flow rate increases. The dry data curve is determined after all the liquid has been expelled from the pores. This dry curve becomes the reference for calculation of the pore distribution. The mean flow pore size is calculated from the pressure at which the wet flow is half of the dry flow [8]. The maximum and the minimum pore sizes are determined from the bubble point and from the point where wet and dry curves converge, respectively.

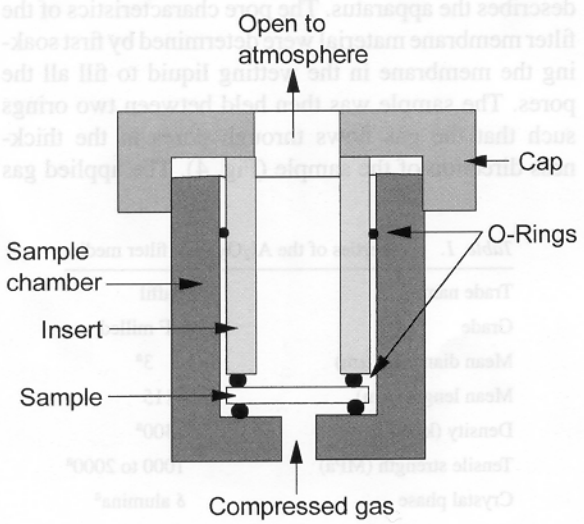

Figure 3. Schematic of filter membrane sample mounted in a Capillary Flow Porometer.

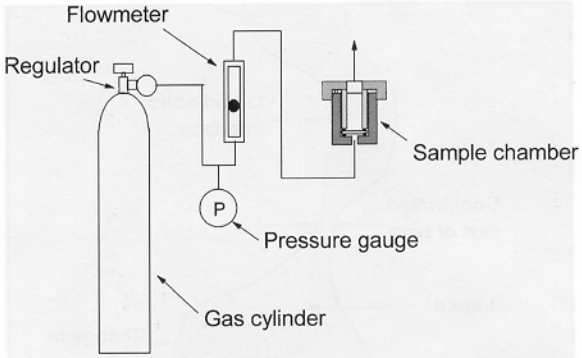

Figure 4. Schematic representation of the experimental apparatus used to generate the flow-pressure curve.

4. Results and Discussion

4.1. *Pore Size*

Equation (5) relates the measured pressure (i.e., pressure difference) at which gas flows through a pore, to the pore diameter. The pore diameter varies along the path of the pore (Fig. 2) and consequently, the pressure required to displace the liquid also varies along the path of the pore. The pressure has its maximum value at the most constricted part of the pore (Fig. 2). Therefore, only when the maximum pressure is reached, gas completely empties the pore and flows through the pore to increase the flow rate at the applied pressure. When characterizing materials for filtration applications, an important advantage of the capillary flow porometry approach is that the pore diameter computed from the measured pressure is the diameter at the most constricted part of the pore [8].

Flow rate versus pressure plots obtained using wet and dry specimens are presented in Fig. 5. It follows from Eq. (5) that the pressure at which flow starts corresponds to the opening of the largest pore. This pressure is known as the bubble point pressure. The largest pore diameter computed using the bubble point pressure is 23 ± 1 μm.

The half-dry curve in Fig. 5 is computed from the dry curve and gives half of the flow rate through the dry sample at a given differential pressure. Pressure at the intersection of the half-dry curve with the wet curve is the mean flow pressure (Fig. 5), which is used to calculate the mean flow pore diameter. The pressure corresponding to the smallest pore diameter is the maximum pressure. The mean flow pore diameter and the smallest detected pore diameter are 2.6 ± 0.1 μm and 1.24 ± 0.06 μm, respectively.

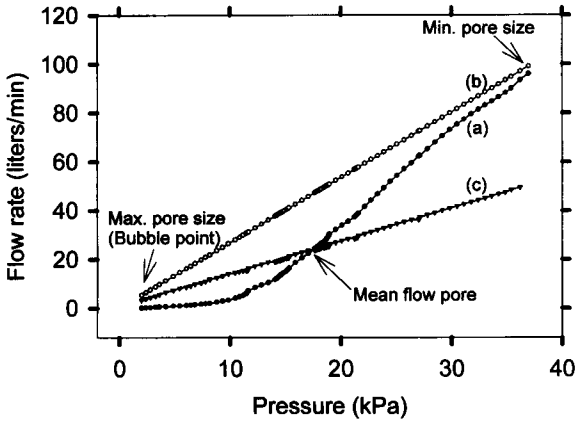

Figure 5. Flow rates of gas through wet and dry specimens as a function of gas pressure: (a) wet curve, (b) dry curve (c) half-dry curve, obtained from (b) by dividing the flow rate by 2.

The cumulative filter flow, as cumulatively obtained upon increasing the pressure during testing, expressed in terms of a percentage of the total flow as a function of pore diameter is shown in Fig. 6. For a given pore size and larger, this graph defines the amount (in percent) of flow through the filter membrane. For example, if we look at the mean flow pore size of 2.56 μm, we can determine from the graph that 50% of the flow is occurring through pores larger than that pore size. This way of expressing pore size and the amount of flow is important in the design of filtration systems since the amount of flow and the size of captured particulate material can be easily correlated.

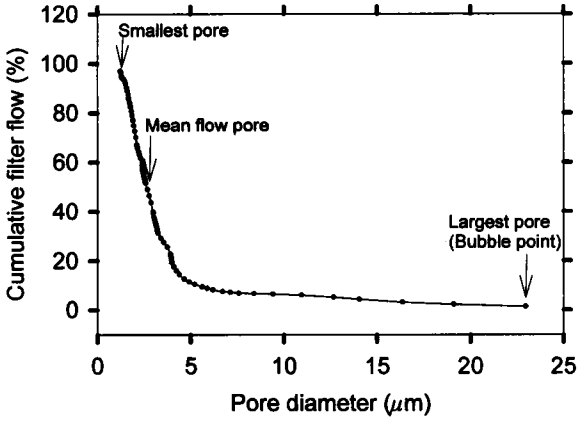

Figure 6. Cumulative filter flow expressed as a percentage versus the pore diameter.

4.2. *Pore Size Distribution*

The pore size distribution is obtained from the flow rates through wet and dry curves. The flow rate through the sample can be expressed in terms of the following equation for viscous flow [8, 11]:

$$Q = [\pi\beta/(128\,\mu l 2p_s)][p_i + p_o][\Sigma_i N_i D_i^4][p_i - p_o]. \tag{6}$$

where Q is the volume flow rate, μ is the viscosity of the gas, p_s is the standard pressure, p_i is the inlet pressure, p_o is the outlet pressure, N_i is the number of pores of diameterD_i, | is the sample thickness and b is a constant.

It follows from this equation that the ratio of flow rate through the wet sample Q_w and the flow rate through the dry sample Q_d measured at the same pressure p_i is independent of pressure [5]. The ratio depends upon pore number and pore diameter [8]. The percentage of flow through pores of any desired size range is given by the area under the curve of the pore distribution function, f, vs. pore diameter. The pore size distribution function, f, is defined as [11].

$$f = -d[100(Q_w/Q_d)]/dD \tag{7}$$

The negative sign on the right hand side of this equation is due to the fact that increase in pore diameter decreases the flow rate. Or conversely, the flow rate will increase as pore size decreases because higher pressures will allow the fluid to permeate through successively smaller pores.

Figure 7 shows the measured pore distribution function vs. the pore diameter. From this graph it was determined that more than 80% of the pores in this specimen range from 2 to 4 μm in size. Scanning electron microscopy shows the porous structure of the alumina fiber filter membrane (Fig. 8).

4.3. *Permeability*

Permeability is the property of a filter medium that permits a fluid to pass through under a pressure differential. The permeability of ceramic membranes depends not only on the type of permeant used, but also on the structure of the porous media. Permeability, k, is given by Darcy's Law [6],

$$k = \frac{Ql\mu}{A \cdot \Delta p}, \tag{8}$$

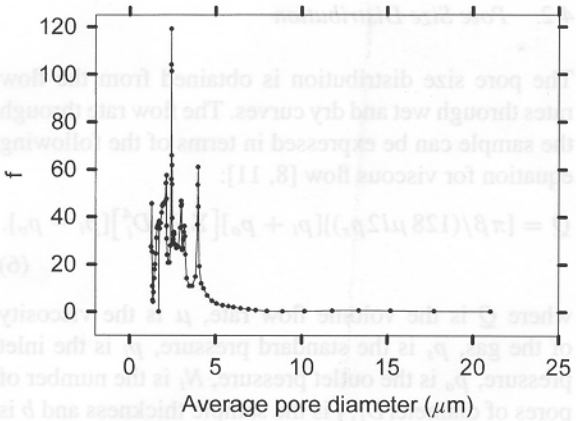

Figure 7. Pore size distribution function versus average pore diameter.

where Q is the gas flow rate in volume per unit time at standard temperature and standard pressure, p_o, μ is the viscosity, | is the specimen thickness, Δp is the pressure differential and A is the sample area.

An alternative form of Darcy's law for ideal gases flowing through a solid porous material was proposed by Collins [19],

$$Qp_a = -\frac{kA}{\mu l}\frac{\left(p_a^2 - p_b^2\right)}{2}, \tag{9}$$

where p_a represents the exit pressure from the material and p_b, the entrance pressure. Taking p_a to be equal to one atmosphere, this equation can then be rearranged, such that

$$k = \frac{8Ql\mu}{\pi D^2\left(p_b^2 - 1\right)} \tag{10}$$

where p_b is measured in atmospheres.

Permeability of any fluid through the filter membrane can be determined by generating the flow versus pressure curve using a dry sample. The dry curve in Fig. 5 gives the flow rate of air through the alumina fiber filter membrane. This data was then used to calculate the permeability of air through the filter

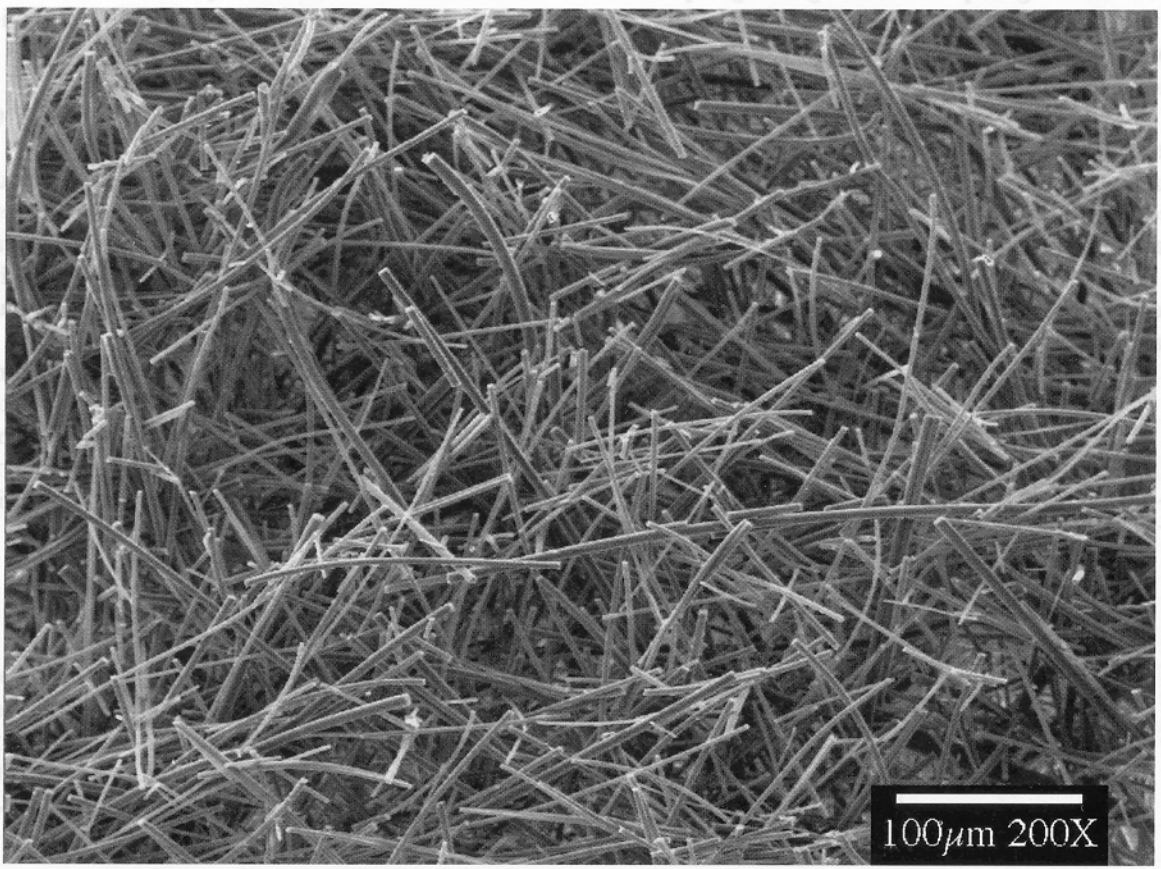

Figure 8. Scanning electron micrograph showing open structure of alumina fiber filter membrane.

membrane using Eq. (10). The physical characteristics of the specimen given in Table 2 and an air viscosity value of 0.0185 cps were used for the calculation. The average Darcy permeability constant, k, is calculated to be $(114 \pm 6) \times 10^{-9}$ cm^2 (11.6 ± 0.6 Darcys).

4.4. *Comparison with Other Filter Membrane Materials*

Filter media used for hot gas filtration can be divided into two general groups, namely, fibrous and granular media. Fibrous media can further be categorized by fabric filters made from polymeric fibers and ceramic or glass fibers.

An example of a fabric material used extensively for hot-gas cleaning in coal-fired power stations was characterized by Jo et al. [20]. The filter material characterized in that study was made from a woven fabric coated with a polyurethane film and was reported to have a wide pore size distribution of 6.09 to 20.5 μm. In comparison, the pore sizes in the present study ranged from 2 to 4 μm. The range of applications available to the woven fabric filter material characterized by Jo et al. is limited not only to particles that are relatively large in size due to its wider pore size distribution but also to applications with relatively low temperature operation because of the limited temperature range in which the polymeric fabric material may be used.

Under the category of ceramic or glass fibers, Ahluwalia et al. [21] characterized the performance of ceramic fiber filters made by Industrial Filter and Pump Manufacturing Company (tradename Fibrosic). The filter materials were characterized to determine mechanical and filtration properties. The Fibrosic filter made from a blend of alumina and aluminosilicate fibers and binder materials had a bulk density of 341 kg/m^3 in comparison to 255 kg/m^3 of the alumina fiber filter material in this study and yet they reported that more than 80% of the pores were in the range of 10 to 90 μm (measured using mercury intrusion porosimetry) in comparison to 2 to 4 μm reported in this work. Also noteworthy, is that despite the higher bulk density, the study by Ahluwalia reported a flexural strength (in three-point bending) of 515.95 ± 129.98 kPa in comparison to 927.55 ± 87 kPa reported for the present alumina fiber filter material in an earlier paper [1].

In another study related to fibrous materials, a hot gas filter was developed by Du Pont Lanxide Composites, Inc., Newark, Delaware, made using a filament winding process using textile grade glass yarn [22]. Their development used a combination of textile and ceramic technologies to produce an all-oxide filter element comprising alumina, cordierite and mullite. The mean pore size and pore size distribution were reported for two versions; one had a mean pore size of 10.5 μm which had greater than 80% of the pores in the range of about 8.5 to 15 μm; the other filter element had a mean pore size of 25 μm and this had greater than 80% of the pores in the range of about 15 to 35 μm. The range of pore size in both versions is considerably wider than the 2 to 4 μm range reported in the present study.

An example of a filter material made with granular or particulate media is the oxide-based hot gas filter element developed by Blasch Precision Ceramics, Albany, New York [23]. Their filter element was made using mullite bonded particulate alumina and had a bulk density of 1840 kg/m^3 (in comparison to a density of 255 kg/m^3 for alumina fiber filter membranes of the present study). They reported the alumina content to be 75 to 85% and the mullite bonding agent to be 20 to 25% by weight of the filter element (in comparison to 9 to 10% by weight of acid phosphate in the present study). The median pore diameter was reported to be 22.4 μm, with greater than 80% of the pores in the range of 7 to 40 μm.

Another example of a particulate based filter membrane is described in a study by Das and Maiti [24]. In this study, the pore structure of a particulate based alumina membrane and the effects of binder content and firing temperature were evaluated for microfiltration applications. The particulate size used in this study was 0.50 μm and the binder was polyvinyl butyral. Benzyl butyl phthalate and polyethylene glycol were also used as plasticizers to aid in the formation of the tape-cast membrane. The binder content ranged from 15 to 27% (compared to 9 to 10% acid phosphate binder in the present study) and the samples were fired at 800°C. Their study showed that the pore size distribution ranged from 0.02 to 0.2 μm irrespective of the binder content. Membranes prepared by the tape-casting technique in the study by Das and Maiti were very thin (50 to 1000 μm) and mechanically very weak despite having densities that ranged from 1750 to 3000 kg/m^3 [24]. This is 7 to 12 times more dense in comparison to the density of the alumina fiber filter membranes in the present study (255 kg/m^3). The

weak mechanical properties of the membrane material prepared by Das and Maiti will prevent the use of their membrane material under vacuum or high fluid pressure.

Several commercial grade hot gas filter materials are also currently available. One example is a ceramic crossflow membrane made by Fairey Industrial Ceramics, Ltd., Staffordshire, U.K. The basis of their α-alumina particulate based ceramic element is a seven channel tubular substrate having an average pore size of 3 μm and a maximum and minimum pore size of 5 and 0.2 μm, respectively [25]. Specific Surface Corporation, Franklin, Massachusetts, has also developed a particulate-based ceramic filter element with a trade name of CandleStac. Their filter element is reported to have a mean pore size of about 15 μm with about 85% of the pores being in the range of 7 to 23 μm [26]. Another example of a commercially available ceramic filter element for hot gas filtration is made by Refractron Technologies, Newark, New York. Their alumina particulate based filter elements have relatively high densities, ranging from 1800 to 2200 kg/m^3 [27] (in comparison to 255 kg/m^3 of the alumina fiber filter material in the present study). Several grades of filter elements are made by Refractron Technologies, having mean pore sizes ranging from 0.08 to 800 μm. There are two general types of filter elements made by Refractron Technologies; (i) membrane coated and (ii) monolithic ceramic. The ceramic filter elements with the finer mean pore sizes (<50 μm) are made with a thin membrane coating bonded to a ceramic core matrix. The membrane performs the filtration duty, while the core matrix acts as the structural support. An example of a membrane coated filter element is a grade called MeAf8, which has a mean pore size of 8 μm with a range from 4 to 14 μm. The monolithic ceramic filter elements are simply the core matrix without the membrane coating. These typically have a much wider pore size distribution, for example, the Af12 grade, has a mean pore size of 12 μm and a range of 4 to 20 μm.

Table 3. Summary of results from capillary flow porometer test[a].

Smallest detected pore pressure (kPa)	37 ± 1.9
Smallest detected pore diameter (μm)	1.24 ± 0.06
Mean flow pore pressure (kPa)	17 ± 0.9
Mean flow pore diameter (μm)	2.6 ± 0.1
Bubble point pressure (kPa)	2 ± 0.1
Bubble point diameter (μm)	26 ± 1
Average Darcy permeability constant, k (10^{-9} cm^2)	114 ± 6

[a]Based on at least three measurements.

5. Conclusions

The pore structure of an alumina-fiber-based hot gas filter membrane containing an acid phosphate binder was characterized using capillary flow porometry. The results are summarized in Table 3. The smallest pore diameter was found to be 1.24 ± 0.06 μm. The largest pore diameter (bubble point pore diameter) was 23 ± 1 μm. The pore size distribution was narrow. Almost all pores ranged from 2 to 4 μm, with the mean flow pore being 2.6 ± 0.1 μm. The permeability of air through the membrane was $(114 \pm 6) \times 10^{-9}$ cm^2.

The narrow pore size distribution means that the alumina fiber filter membrane characterized in the present study is suitable for microfiltration of gases containing fine (1–10 μm) particles.

References

1. J.A. Fernando and D.D.L. Chung, J. Mater. Sci. **36**, 5079 (2001).
2. Y.M. Jo, R.B. Hutchison, and J.A. Raper, Powder Tech. **91**, 55 (1997).
3. S.C. Mitchell, Hot Gas Particulate Filtration (IEA Coal Research, 1997).
4. N. Das and H.S. Maiti, J. Membrane Sci. **140**, 205 (1998).
5. L.J. Zeman and A.L. Zydney, *Microfiltration and Ultrafiltration* (Marcel Dekker, 1996).
6. K. Venkataraman, W.T. Choate, E.R. Torre, R.D. Husung, and H.R. Batchu, J. Membrane Sci. **39**, 259 (1988).
7. E. Jakobs and W.J. Koros, J. Membrane Sci. **124**, 149 (1997).
8. A.K. Jena and K.M. Gupta, J. Power Sources **80**, 46 (1999).
9. R. Rocek and P. Uchytil, J. Membrane Sci. **89**, 119 (1994).
10. A. Bottino, G. Capannelli, P. Petit-Bon, N. Cao, M. Pegorao, and G. Zoia, Sep. Sci. Technol. **26**, 1315 (1991).
11. V. Gupta and A.K. Jena, Adv. in Filt. and Separ. Tech. **13b**, 833 (1999).
12. S. Munari, A. Bottini, P. Moretti, G. Capannelli, and I. Becchi, J. Membrane Sci. **41**, 69 (1989).
13. F.P. Cuperus and C.A. Smolders, Adv. Coll and Interface Sci. **34**, 135 (1991).
14. K.J. Kim, A.G. Fane, R.B. Aim, M.G. Liu, G. Jonsson, I.C. Tessaro, A.P. Broek, and D. Bargeman, J. Membrane Sci. **87**, 35 (1994).
15. K.S. McGuire, D.R. Lloyd, and G.B. Lim, J. Membrane Sci. **99**, 127 (1995).
16. P. Schneider and P. Uchytil, J. Membrane Sci. **95**, 29 (1994).
17. P. Uchytil, J. Mater. Sci. **31**, 6293 (1996).
18. A.S. Kim, S. Bengtsson, and R. Warren, Composites Sci. Tech. **47**, 331 (1993).
19. R.E. Collins, *Flow of Fluids Through Porous Materials* (Chapman and Hall, 1961).

20. Y.M. Jo, R. Huchison, and J.A. Raper, Waste Management & Research **14**, 281 (1996).
21. R.K. Ahluwalia, V.J. Novick, L. Zhang, M.P. Sutaria, and J.P. Singh, *Advanced Coal-Based Power and Environmental Systems Conference*, Federal Energy Technology Center, Morgantown, West Virginia, July 21–23, 1998.
22. G.D. Forsythe and E.S. Connolly, *Advanced Coal-Based Power and Environmental Systems Conference*, Federal Energy Technology Center, Morgantown, West Virginia, July 21–23, 1998.
23. J. Bolebruch and D.A. Larsen, *Advanced Coal-Based Power and Environmental Systems Conference*, Federal Energy Technology Center, Morgantown, West Virginia, July 21–23, 1998.
24. N. Das and H.S. Maiti, J. Membrane Sci. **140**, 205 (1998).
25. Fairey Industrial Ceramics, Ltd., Product Information Web Site.
26. Specific Surface Corporation, Product Information Sheet, 2000.
27. Refractron Technologies Corp., Product Information Sheet, Thomas Publishing Company, New York, 1998.